SURAT PENCATATAN CIPTAAN

Dalam rangka pelindungan ciptaan di bidang ilmu pengetahuan, seni dan sastra berdasarkan Undang-Undang Nomor 28 Tahun 2014 tentang Hak Cipta, dengan ini menerangkan:

Nomor dan tanggal permohonan	:	EC002025036689, 7 April 2025
Pencipta		
Nama	:	**Dr. Dahlia Sutanto, drg., SpPros., drg. Silvia Naliani, SpPros.,MKG. dkk**
Alamat	:	Jl. Golf Barat VIII No. 17, RT. 001 RW. 013, Arcamanik, Kota Bandung, Jawa Barat, 40293
Kewarganegaraan	:	Indonesia
Pemegang Hak Cipta		
Nama	:	**Universitas Kristen Maranatha**
Alamat	:	Jl. Prof.drg. Surya Sumantri, M.P.H. No.65, Sukajadi, Kota Bandung, Jawa Barat, 40175
Kewarganegaraan	:	Indonesia
Jenis Ciptaan	:	**Jurnal**
Judul Ciptaan	:	**Comparison of Collagen Fiber and Callus Deposition on Geopolymer-Carbonated Hydroxyapatite Nanocomposite Doped with Magnesium and Strontium on Days 14 and 28 Using Masson's Trichrome**
Tanggal dan tempat diumumkan untuk pertama kali di wilayah Indonesia atau di luar wilayah Indonesia	:	5 Maret 2025, di Tallinn Estonia
Jangka waktu pelindungan	:	Berlaku selama hidup Pencipta dan terus berlangsung selama 70 (tujuh puluh) tahun setelah Pencipta meninggal dunia, terhitung mulai tanggal 1 Januari tahun berikutnya.
Nomor Pencatatan	:	000876950

adalah benar berdasarkan keterangan yang diberikan oleh Pemohon.
Surat Pencatatan Hak Cipta atau produk Hak terkait ini sesuai dengan Pasal 72 Undang-Undang Nomor 28 Tahun 2014 tentang Hak Cipta.

a.n. MENTERI HUKUM
DIREKTUR JENDERAL KEKAYAAN INTELEKTUAL
u.b
Direktur Hak Cipta dan Desain Industri

Agung Damarsasongko,SH.,MH.
NIP. 196912261994031001

LAMPIRAN PENCIPTA

No	Nama	Alamat
1	Dr. Dahlia Sutanto, drg., SpPros.	Jl. Golf Barat VIII No. 17, RT. 001 RW. 013 Arcamanik, Kota Bandung
2	drg. Silvia Naliani, SpPros.,MKG.	GG. Sukasingkir No. 22/66, RT. 009 RW. 004 Cicendo, Kota Bandung
3	Teresa Lucretia Maria Astari, dr., M.Kes.	Maltra Residence E4, RT. 002 RW. 007 Andir, Kota Bandung

Original Article

Comparison of Collagen Fiber and Callus Deposition on Geopolymer-Carbonated Hydroxyapatite Nanocomposite Doped with Magnesium and Strontium on Days 14 and 28 Using Masson's Trichrome

Dahlia Sutanto[1] 🔗 Silvia Naliani[1] Teresa Lucretia[2]

[1] Department of Prosthodontics, Faculty of Dentistry, Maranatha Christian University, Bandung, West Java, Indonesia

[2] Department of Histology, Faculty of Medicine, Maranatha Christian University, Bandung, West Java, Indonesia

Address for correspondence Dahlia Sutanto, drg., SpPros, Department of Prosthodontics, Faculty of Dentistry, Maranatha Christian University, Jalan Surya Sumantri 65, Bandung, West Java 40132, Indonesia (e-mail: dahlia.sutanto@dent.maranatha.edu).

Abstract

Objectives   This study aimed to evaluate collagen fiber deposition and callus formation on geopolymer-carbonated hydroxyapatite (CHA) nanocomposites-doped with magnesium (Mg) and strontium (Sr) on days 14 and 28 in the tibia of New Zealand rabbits.

Materials and Methods   Geopolymer-CHA-Mg-Sr nanocomposite samples with a diameter of 3 mm and a height of 6 mm were placed in the tibia of eight New Zealand rabbits. Experimental subjects were randomly divided into two groups to evaluate collagen fiber deposition and callus formation on days 14 and 28 histomorphologically.

Statistical Analysis T-test was performed, and $p < 0.05$ was considered statistically significant using Minitab version 13.

Results   There was no significant difference in collagen deposition and callus formation on the geopolymer-CHA-Mg-Sr surface on days 14 and 28 with p-values 0.075 and 0.842, respectively.

Conclusion   Geopolymer-CHA-Mg-Sr is biocompatible, bioinert, and osteoconductive, and its mechanical properties meet the dentin standard values for hardness, while the modulus of elasticity, compressive, and tensile strength meets the enamel standard values.

Keywords
► collagen fiber deposition
► callus
► geopolymer-CHA-Mg-Sr
► Masson's trichrome

Introduction

Dental implants are the primary treatment option for patients who have lost teeth due to caries, periodontal disease, failure of endodontics, or injuries. Dental implants can support partial, complete, or fixed dentures to improve retention, stabilization, masticatory efficiency, and quality of life. The most frequently used implant materials are metal and ceramic, considering that titanium and ceramic's biocompatibility and mechanical properties are excellent[1–4]; however, titanium does not have bioactive properties that promote osteointegration or prevent infection, while the natural surface structure of ceramics does not have good osseointegration capabilities.[5–7] Titanium implants cause a grayish color, especially in the anterior area where the gingival tissue is very thin, causing a galvanic reaction that occurs after contact with saliva and fluoride, and an inflammatory response and bone resorption were also found to be

induced due to titanium particles.[4] It has been reported that at least 5% of dental implant fractures arise due to fatigue over the past few decades.[8] In terms of biological properties, the mechanical properties of implants such as the elastic modulus values of titanium ($2,222.7 \pm 277.6$ MPa) and zirconia (90 GPa) exceed the elastic modulus values of enamel and dentin, respectively ($1,338.2 \pm 307.9$ and $1,653, 7 \pm 277.9$ MPa).[5]

The main factor that determines the success of dental implantation is osseointegration, a biological process that is the stable anchorage in the bone tissue achieved by direct bone-to-implant contact without the presence of fibrous tissue at the bone–implant interface. This process involves a complex relationship between the biocompatibility of the biomaterial properties and the mechanical environment in which the implant is placed.[9,10]

The osseointegration mechanism of titanium/titanium alloy implants cannot form an interfacial bond with bone without a micromechanical interlock. Therefore, surface characterization is needed to encourage bone growth and increase interfacial bonds, such as coating as a mediator to osteoblast cells.[1,7,11] However, the coating does not produce perfect osseointegration, such as the dissolution of calcium phosphate and the release of the coating material.[12–15]

Considering the current osseointegration capabilities of metal and ceramic implants, it is necessary to develop implant materials that can stimulate osseointegration with inorganic materials that resemble the chemical structure of bones and teeth without coatings, nonmetal elements with ceramic-like properties. Osseointegration with nonmetallic implants made from inorganic materials that resemble the chemical structure of bones and teeth prevents osseointegration failure caused by the release of coating materials such as hydroxyapatite which is often used on the surface of titanium implants to stimulate osseointegration, and their bioactive and osteoconductive capabilities can stimulate bone growth on the implant surface which promotes osseointegration. Excellent corrosion resistance in the physiologic environment, acceptable strength, high wear resistance, and a modulus of elasticity similar to bone minimize bone resorption around the implant, thus preventing implant failure.[5–7]

In 1978, Joseph Davidovits reported geopolymers as an inorganic material with ceramic-like properties. Geopolymer is a ceramic, inorganic polymer formed through a dissolution and precipitation process from aluminosilicate precursors.[16,17]

The advantages of geopolymer materials include excellent mechanical properties such as high compressive strength ranging from 52 to 75 MPa, bioactive properties, biocompatibility, being suitable for hard tissue prostheses, and being environmentally friendly.[18–23]

Tippayasam et al reported the bioactive and biocompatible properties of geopolymers. They accelerated the formation of new bone tissue by promoting the genetic activity of bone regulatory cells.[24]

The minerals in bones and teeth consist mostly of hydroxyapatite. In addition to Ca and phosphate (PO_4^{3-}), various inorganic substances (carbonate [CO_3^{2-}], magnesium [Mg], Na, K, Sr, etc.) are present in bone minerals in the form of solid solutions.[25]

Mg and CO_3^{2-} are minor elements compared with Ca and PO_4^{3-}, but are essential elements in calcified tissues (enamel, dentin, bone).[26] Strontium (Sr) is an essential trace element in the human body with a content of more than 0.01 wt.% in bones.[25,27,28] According to Yang et al and Saidak and Marie, Sr can increase osseointegration both in vitro and in vivo.[29,30] Sr has the same chemical and physical properties as Ca.[31]

Although geopolymers are used as stand-alone materials with suitable properties, combination with other materials is likely another way to improve their properties.[24]

One of the determining factors for the success of a material is the presence of unimpeded bone growth onto or across the surface of the material sample at the initial stage of the bone healing sequence, which is characterized by new bone tissue forming on the surface of the material sample.[12,32,33]

Bone healing or wound healing after implantation is as such the process of fracture healing that recapitulates bone development,[12,32,33] and the stages of bone healing consist of hematoma, acute inflammation, granulation tissue formation, callus formation, and remodeling.[34,35]

The formation of woven bone is essential for bone repair and regeneration success. Histologically, woven bone is an arrangement of osteoblast cells and collagen fibers which can be observed through Masson's trichrome staining. Collagen fibers are irregular and random fibers that only experience light calcination and are found during bone growth and development and hard callus in bone fractures.[36]

Among the various dental materials, an implant system must have essential requirements, including biological, mechanical, and morphological compatibility, considering that the implant surface is in direct contact with hard and soft tissues.

Based on this background, nonmetallic implant materials with mechanical properties close to the mechanical properties of tooth tissue, bioactive, and osteoconductive capabilities that stimulate bone growth on the implant surface which promote osseointegration are needed.

In this research, we performed in vivo histomorphologically to evaluate collagen fiber deposition and callus formation.

Materials and Methods

Sodium hydrogen carbonate, calcium nitrate tetrahydrate, diammonium hydrogen phosphate, magnesium chloride hexahydrate, strontium chloride hexahydrate, 25% ammonia solution, and sodium hydroxide used in this study were produced by Merck. Sodium silicate was obtained from Sigma-Aldrich. Kaolin was prepared from the ceramic center of the Indonesian Ministry of Industry, and metakaolin was obtained by heating kaolin in a furnace at 800°C for 8 hours.

Synthesis of Carbonate Apatite
The ammonia solution was dropped into the 0.1 M calcium nitrate tetrahydrate solution, stirred with a magnetic stirrer until the pH reached 9, followed by the addition of 100 mL of

diammonium hydrogen phosphate 0.06 M and 100 mL of sodium hydrogen carbonate 0.06 M. The pH of the mixture was adjusted again by dripping the ammonia solution until it reached 9. The solution was kept at room temperature (RT) for 12 hours. The precipitate was separated and dried in an oven at 80°C for 30 minutes. Samples were calcined from 25°C to 700°C for 2 hours. Nanoparticle powder was ground with a mortar and pestle.

Synthesis of Mg- and Sr-Doped Carbonated Hydroxyapatite

The first stage in the synthesis of Mg- and Sr-doped carbonated hydroxyapatite (CHA) starts from preparing 100 mL of 0.01 M $MgCl_2$ and 100 mL of 0.01 M $SrCl_2$ solutions. This $MgCl_2$ solution will be used as a source of Mg in apatite carbonate nanoparticles. This solution was made by preparing 100 mL of aqua demineralized (DM) as a solvent, then 0.203 g of $MgCl_2$ was dissolved in the solvent and stirred with a magnetic stirrer until completely dissolved, and the pH of the solution was increased by dripping ammonia solution into the solution until it reached 9. Likewise, $SrCl_2$ solution was made by preparing 100 mL of aqua DM as a solvent, then 0.266 g of $SrCl_2.4H_2O$ salt is dissolved in the solvent and stirred with a magnetic stirrer until completely dissolved, and the pH of the solution was increased until it reached 9.

Five milliliters of previously prepared $MgCl_2$ 0.01 M and $SrCl_2$ 0.01 M solutions at pH 9 were added dropwise into a mixture containing calcium nitrate tetrahydrate, diammonium hydrogen phosphate, and sodium hydrogen carbonate as mentioned earlier. pH of the mixture was adjusted again by dripping the ammonia solution until it reached 9. The solution was kept at RT for 12 hours, and the precipitate was separated and dried in an oven at 80°C for 30 minutes. Samples were calcined from 25°C to 700°C for 2 hours. Nanoparticle powder was ground with mortal and pestle, thus producing a fine and white powder.

Preparation of Geopolymer

The geopolymer samples were prepared by mixing metakaolin with an alkali activator consisting of sodium silicate and 12 M NaOH with a w/w ratio of 2:1. The resulting paste was poured into an acrylic mold and kept at RT for 30 minutes and dried in an oven at 80°C for 20 hours, and the samples were allowed to cool at RT.

Preparation of Geopolymer-CHA-Mg-Sr Nanocomposite

CHA-Mg-Sr powder was mixed with metakaolin in a 1:1 ratio and subsequently added dropwise to an alkali activator, which was a mixture of sodium silicate and a 12 M NaOH solution and stirred until it was homogeneous to form paste-like sample. Furthermore, the mixture was poured into an acrylic mold, kept at RT for 30 minutes, and dried in an oven at 80°C for 20 hours, and the samples were allowed to cool at RT.

Characterization

Biological characterization was performed using the trypan blue method for cytotoxicity tests to verify the morphology and viability of fibroblast cells. Geopolymer-CHA-Mg-Sr samples were washed for 96 hours in DM water before being subjected to cytotoxicity tests using an H7KT26012 shaker (Thermo Scientific).

Fibroblast cells were cultured in RPMI 1640 Medium (Gibco, United States). Geopolymer-CHA-Mg-Sr samples in cylinder form were evaluated in duplicate with a size of 3 mm × 6 mm. Fibroblast cells were placed at 100% cells/well in six wells and incubated for 24, 48, and 72 hours at 37°C. Each well was washed with 1 mL of PO_4^{3-}-buffered saline solution, pH 7.4 (Gibco, United States). One milliliter of trypsin (Gibco, Denmark) was dropped into each well, then incubated for 5 minutes. Cells were quantified with a hemocytometer (Neubauer Improved, Marienfeld, Germany), and cell morphology was evaluated using a Motic Inverted Microscope (Olympus CK40) with a 10-MP resolution camera.

Fourier transform infrared (FTIR) spectroscopy is a characterization technique that can provide information about the types of molecules present in the sample and their concentration levels. The resulting spectrum describes the absorption and transmission of molecules, producing a molecular fingerprint of the sample.

FTIR measurements were recorded with KBr pellets on a Prestige 21 Shimadzu. Sample shuttle measurements were performed to insert samples and background scans. The spectrum was measured at a resolution of 4 cm^{-1} with the number of scans 40 and at a wavelength of 4,500 to 400 cm^{-1}.

Energy dispersive X-ray (EDX) analysis, also known as EDS or *EDAX*, is an X-ray technique used to identify the elemental composition of materials. Sample compositions were measured using Hitachi SU3500 SEM-EDX spectroscopy. EDAX characterization was used to confirm the presence of Mg and Sr in samples.

Sample hardness testing was performed using the Shimadzu Micro Vickers Hardness Tester HMV-G21 series. The indentation load of 100 gf was applied with a holding time of 15 seconds. Nanocomposite specimens were made in cylinders with 5 mm × 6 mm dimensions, each sample was indented on three different points.

Diametral tensile strength, compressive strength, and three-point bending tests were performed using Shimadzu AGS-X series. Diametral tensile strength specimens are provided in cylinder form with a diameter of 6 mm and a thickness of 3 mm. Measurements were performed using a 1 kN load cell, with a crosshead speed 1 mm/s. Compressive strength specimens are provided in cylinder form with a diameter of 4 mm and a thickness of 6 mm.

Specimens for three points bending were prepared with a bar of 25 mm × 5 mm × 2.0 mm with load cell 1 kN, 1 mm/s, and a span of 10 mm. For the diametral tensile strength test, the specimens were compressed diametrically, inducing tensile stress in the material along the plane of force application.

Study Design

In this study, we used New Zealand rabbits considering that rabbits are medium-sized animals that are often used as

animal model for implant biomaterial research in bone. This is in part due to their ease of handling and size, as well as international standards that designate species such as dogs, sheep, goats, pigs, or rabbits as suitable for testing implantation of materials in bone. Although rabbits have limitations in terms of similarities to human bone characteristics compared with dog, pig, and sheep, rabbits have a bone composition moderately similar to human bones and the rabbit remains a very popular choice of species for the testing of implant materials in bone. Rabbits are often used to screen implant materials before testing on higher level animals.

In this study, eight clinically healthy 6-month-old male New Zealand rabbits weighing between 3.0 and 3.5 kg were used. Animal selection, management, and surgery protocol were approved by the Animal Care and Use Committee of Bogor Agricultural Institute University numbered 151/KEH/SKE/VIII/2019. The experimental segment of the study was started after an adaptation period of 2 weeks.

Experimental subjects were randomly assigned to two groups to evaluate collagen fiber deposition and callus formation capability around samples. One group of four rabbits was evaluated for 14 days, and the other group of four rabbits was assessed for 28 days.

Surgical Procedure

The geopolymer-CHA-Mg-Sr samples, with a diameter of 3 mm and a length of 6 mm were thoroughly rinsed with sterile saline and positioned in tibia metaphysis. After incision and preparation of bone defects using a low-speed drill with a 3-mm diameter and 6-mm length, with continuous irrigation, the samples were left to heal in a submerged position.

To maintain hydration, all animals received a constant-rate infusion of lactated Ringer's solution while anesthetized. Analgesic Fortis (Dong Bang Co, Ltd, GYeonggi-do, Korea) 1.1 mg/kg and Genta-100 (Interchemie werken "De Adelaar" BV, Venray, Holland) 10 mg/kg were administered via intramuscular injection after surgery and following 3 days after surgery, topical application of Nebacetin ointment (Pharos, Jakarta) in the wound area until healed is presented in ►Fig. 1.

Animal Euthanasia and Retrieval of Specimens

Rabbits were euthanized on days 14 and 28 using an overdose of pentobarbital sodium and phenytoin 0.5 mL/kg body weight by intravenous injection. Subsequently, the tibia was dissected, and a segment of metaphysis $\sim$2.0 cm in length comprising the sample was obtained for histological study. All specimens were fixed in 10% neutral buffered formalin solution for 24 hours and followed by histological preparation.

Histological Preparation

Samples were fixed for 24 hours in buffered formalin and decalcified for 96 hours with a commercial EDTA-hydrochloric acid mixture (Surgipath Decalcifier II, Leica Biosystem, United States). Bone segments were cut lengthwise with the sample plane, then dehydrated using ascending concentrations of alcohol, followed by absolute ethanol and xylol, and specimens were embedded in paraffin wax (Thermo Scientific Histoplast, Cheshire, UK).

The paraffin wax-embedded samples were cut into 5-μm-thick sections using a microtome, labeled, and mounted on poly-L-lysine-coated glass slides (Sigma-Aldrich, Gillingham, UK). Sections were deparaffinized and rehydrated by rinsing with xylene for 10 minutes, industrial methylated spirit for 5 minutes, and tap water for 5 minutes. Sections were stained with routine hematoxylin and eosin and Masson trichrome to identify locations of collagen fiber deposition and callus formation.

Results

Cell viability of all samples showed a value higher than 80%. It is noteworthy to mention here that apparently all samples
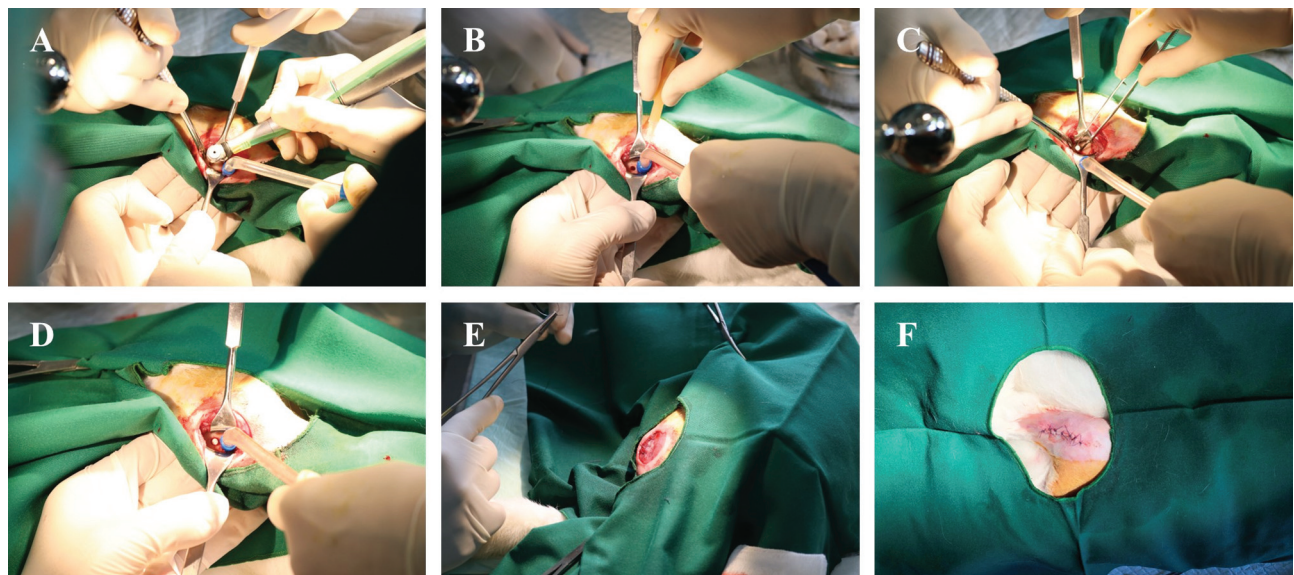

Fig. 1 Incision and preparation of bone defects (A), bone defect with 3 mm in diameter and 6 mm of depth (B), sample was positioned in tibia metaphysis (C), sample was in submerged position in bone (D), the wound was closed with resorbable white sutures and allowed to heal (E, F).
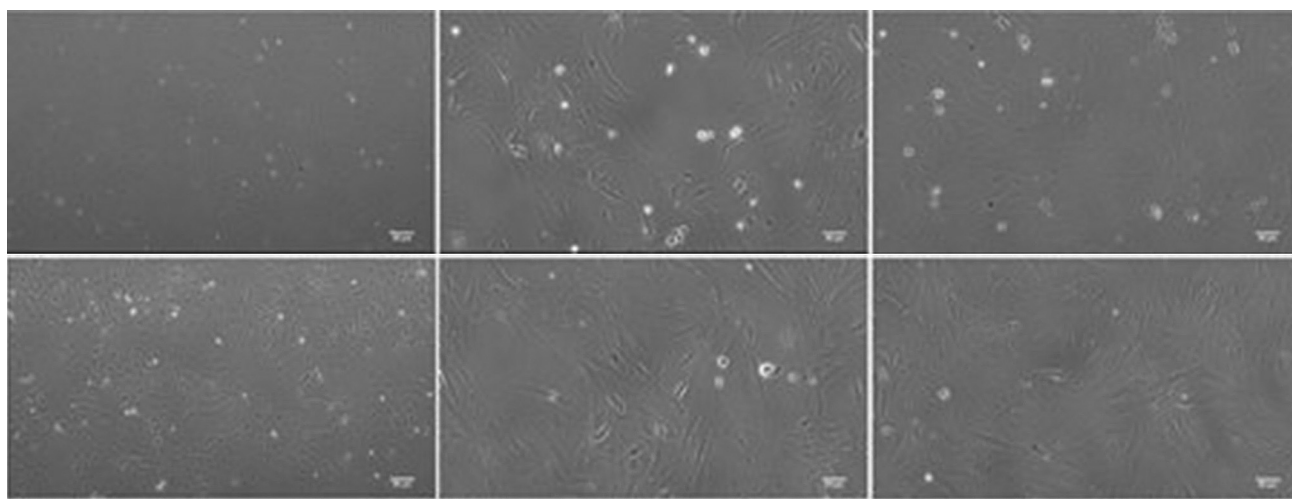
Fig. 2 Microscope images of mouse embryonic fibroblasts after 24, 48 and 72 hours incubation on control group (top) and geopolymer-CHA-Mg-Sr) nanocomposite (bottom). The bar denotes 50 μm. CHA, carbonated hydroxyapatite.
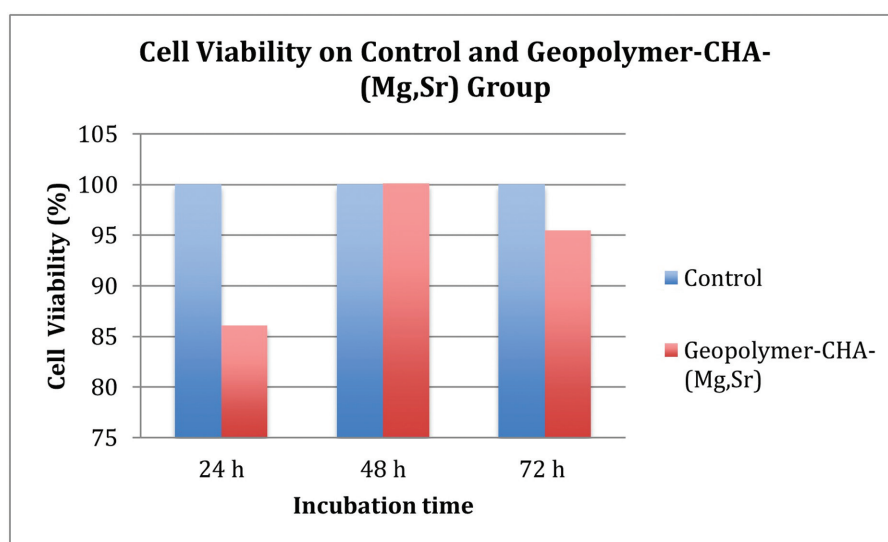

Fig. 3 Cell viability of mouse embryonic fibroblasts on control and geopolymer-CHA-Mg-Sr group after 24, 48, and 72 hours incubation. CHA, carbonated hydroxyapatite.

were biocompatible. After 72 hours of incubation, the cell viability reached higher than 90%, calculated 95.7% for geopolymer-CHA-Mg-Sr. The cell viability of the samples is presented in ►**Figs. 2** and **3**.

FTIR spectra in ►**Fig. 4** showed a peak at 3,453 in samples containing geopolymer, indicating the O–H stretching vibration from adsorbed water, whereas in metakaolin, these peaks are relatively low. Geopolymer sample shows peaks at 1,465 cm^{-1} that indicate the formation of sodium carbonate because of the reaction between an excess of NaOH and CO_2 in the air. The CHA, Mg, and Sr trace elements are challenging to observe from FTIR, as most peaks overlap with geopolymer.

The EDAX spectrum shows the presence of added Mg and Sr elements in nanocomposite as shown in ►**Fig. 5** supporting the FTIR results. The EDAX spectrum of geopolymer-CHA-Mg-Sr only shows a small Sr peak, while the Mg peak is difficult to observe. However, the FTIR spectrum shows Mg-

O and Sr-O vibrations, so it can be concluded that Mg and Sr have successfully incorporated into CHA.

Mechanical Characterization

The mean value obtained from physical characterization was reported as mean ± standard derivation. This was followed by a descriptive analysis of hardness, compressive strength, diametral strength, and modulus of elasticity values against standard values for enamel and dentin.

Geopolymer-CHA-Mg-Sr nanocomposites demonstrated hardness values (80.43 ± 11.36 Vickers hardness number [VHN]) that had not yet reached the enamel standard value of 274.8 VHN, but they met the range of dentine value (53 ± 63 VHN), the compressive strength value (71.21 ± 14.65 MPa) was higher than those in enamel (38.4–86 MPa) but lower than dentine standard value (163.1 ± 224.3 MPa).[37,38] Geopolymer-CHA-Mg-Sr nanocomposites demonstrated a tensile strength value (11.45 ± 3.40 MPa) higher than the enamel standard
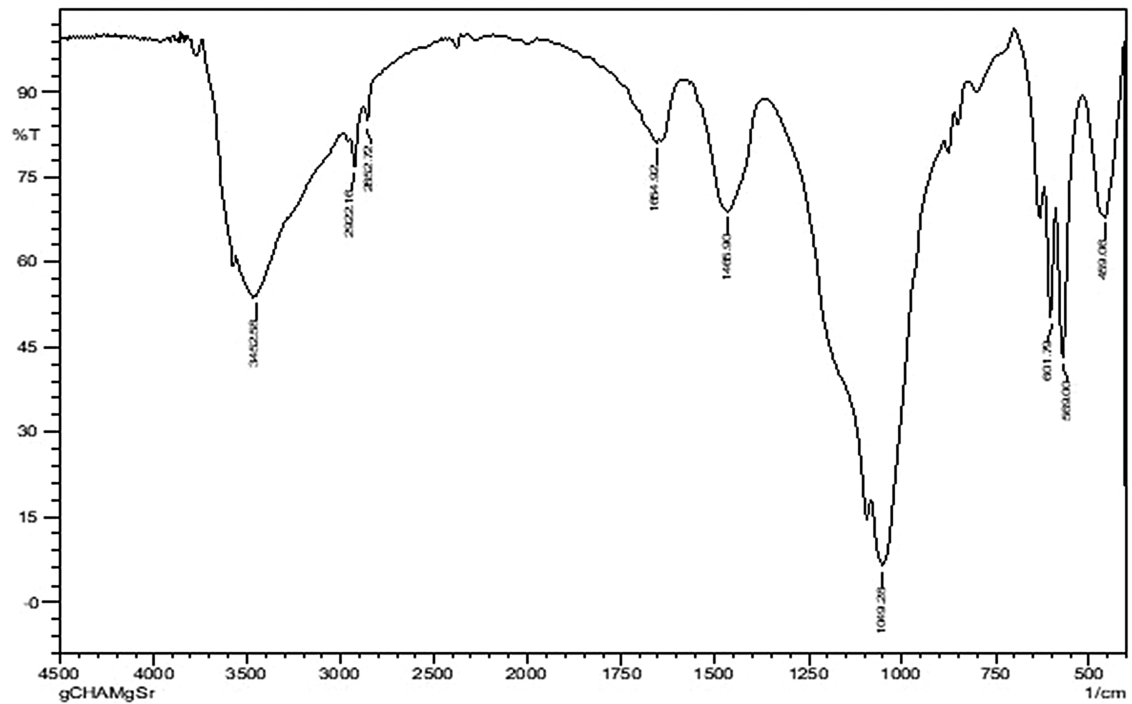
Fig. 4 Fourier transform infrared (FTIR) spectra of geopolymer-CHA-Mg-Sr nanocomposite. CHA, carbonated hydroxyapatite.
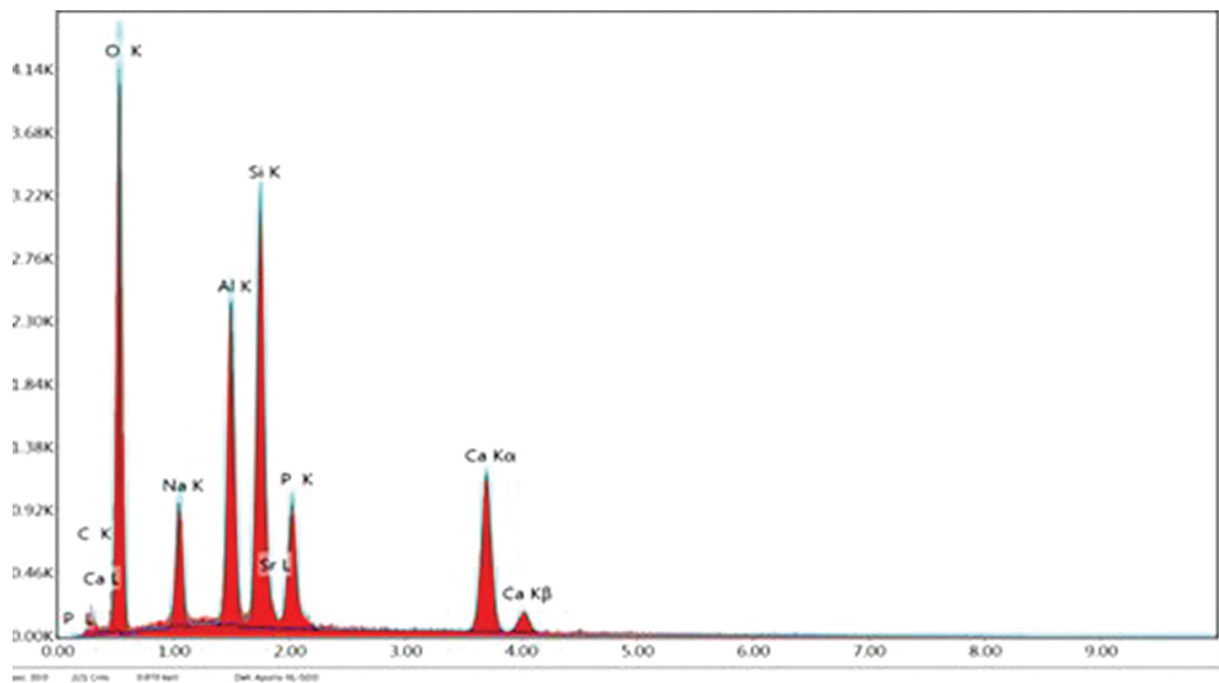

Fig. 5 EDAX spectrum of geopolymer-CHA-Mg-Sr. CHA, carbonated hydroxyapatite.

value of 8 to 35 MPa but lower than that of dentine (31–104 MPa). Modulus elasticity (7,193.03 ± 1,646.1 MPa) was higher than the enamel standard value (1,030.3–1,646.1 MPa) and lower than the dentine standard value (15,000 MPa) as presented in ►**Tables 1** and **2**.[37,38]

Collagen Fiber Deposition and Callus Formation

Image measurements for implant circumference length, new collagen tissue circumference length, implant area, and newly

formed callus/bone area used Fiji software (Image J). Images were taken using an Optilab v 2.2 device attached to a light microscope Olympus CX23. All images were taken with ×4 objective lens magnification.

Data analysis was performed by comparing the percentage of new collagen fibers divided by the circumferential length of the implant material in the area where the synthetic implant material meets the bone on days 14 and 28. Likewise, the percentage of callus tissue was divided by the

Table 1 The mean mechanical properties of geopolymer-CHA-Mg-Sr nanocomposite against enamel standard values

Material	Hardness (VHN) 274.8[a]	Compressive strength (MPa) 38.4–86[a]	Tensile strength (MPa) 8–35[a]	Modulus elasticity (MPa) 1,030.3–1,646.1[a]
Geopolymer-CHA-Mg-Sr	80.43 ± 11.36	71.21 ± 14.65	11.45 ± 3.40	$7,193.03 \pm 643.23$

Abbreviations: CHA, carbonated hydroxyapatite; VHN, Vickers hardness number.
[a]Enamel standard value.[37,38]

Table 2 The mean mechanical properties of geopolymer-CHA-Mg-Sr nanocomposite against dentin standard values

Material	Hardness (VHN) 53–63[a]	Compressive strength (MPa) 163.1–224.3[a]	Tensile strength (MPa) 31–104[a]	Modulus elasticity (MPa) 15,000[a]
Geopolymer-CHA-Mg-Sr	80.43 ± 11.36	71.21 ± 14.65	11.45 ± 3.40	$7,193.03 \pm 643.23$

Abbreviations: CHA, carbonated hydroxyapatite; VHN, Vickers hardness number.
[a]Dentin standard value.[37,38]

circumferential length of the implant material in the area where the synthetic implant material meets the bone on days 14 and 28 as presented in ►Fig. 6A.

The data were processed by statistical test using the t-test, where p-value less than 0.05 was considered statistically significant. The percentage of collagen tissue deposition formed on geopolymer-CHA-Mg-Sr on days 14 and 28, respectively, were 63.98 and 72.45%, while the rate of callus formation formed on geopolymer-CHA-Mg-Sr on the 14th and 28th days, respectively, were 8.13 and 7.80%.

A statistical test using the t-test showed no significant difference in collagen deposition and callus formation on geopolymer-CHA-Mg-Sr surface on days 14 and 28, with p-value of 0.075 and 0.842, respectively, as presented in ►Tables 3 and 4.

Discussion

The minerals in bones and teeth consist mostly of hydroxyapatite. In addition to Ca and PO_4^{3-}, various inorganic substances (CO_3^{2-}, Mg, Na, K, Sr, etc.) are present in bone minerals in the form of solid solutions.[25]

Enamel on teeth is the most hardest and mineralized tissue of the human body, consisting of 96% CHA crystals, while dentin is a hard tissue composed of $\sim$70% hydroxyapatite crystals.[37,39]

Based on the mineral in teeth, the development of geopolymers in this research uses minerals such as those in bones and teeth, namely calcium phosphate from apatite carbonate, Mg, and Sr to simulate the chemical properties of bones and teeth and to expand the application of dental materials that require cell integration to improve osseointegration.[16,17,40–42]

Geopolymer which has bioactive and biocompatible properties can accelerate the formation of new bone tissue by promoting osteoblast cell activity.[24]

Osseointegration is related to the activity of osteoblast cells both on the bone surface in contact with the implant and new bone formation.[12] The process of forming collagen fiber and callus, which begins new bone formation, is influenced by the role of Mg and Sr. Mg increases the differentiation of preosteoblasts into osteoblasts, stimulates osteoblast cell proliferation, and maintains vascular function by inducing the production of endothelial cells in the proliferation phase, which lasts from several weeks to months after placement of the geopolymer-CHA-Mg-Sr sample.[43–48]

Mg binds to integrin subunits and increases integrin expression in osteoblasts. Integrin α5β1 selectively binds to fibronectin to bind to cells and activates focal adhesion kinase, which has an important role in integrating integrin signals to activate MAPKS in increasing osteogenesis by activating Runx2 which plays a role in osteogenic differentiation.[31]

Sr plays a role in activating the Ca-sensing receptor (CaSR) signaling pathway which encourages proliferation and differentiation of osteoblast cells and at the same time, Sr induces apoptosis of the resulting osteoclast cells. Sr can inhibit osteoclast activity and stimulate osteoblast activity.[43–48]

The mechanism of Sr is similar to Ca, binding to Ca receptors in bones. Sr and Ca bind to CaSR to promote osteogenesis, when CaSR is activated, divalent cations increase, and intracellular signaling pathways begin to activate G-proteins which cause activation of tyrosine kinase, phospholipase C, and adenylate cyclase which triggers phosphorylation and activates MAPKS, Ras/Raf /MEK/ ERK1/2 in increasing osteogenesis by activating Runx2 which plays a role in osteoprogenitor proliferation and osteoblast maturation.[49]

The proliferation phase takes place on days 14 and 28, during which there are many major cellular and biological activity processes, especially angiogenesis. Angiogenesis is necessary during osseointegration, and osseointegration will not be successful without angiogenesis.[35]

The wound healing phase is the same as bone formation, consisting of the hemostasis, inflammatory, proliferation, and remodeling phases.
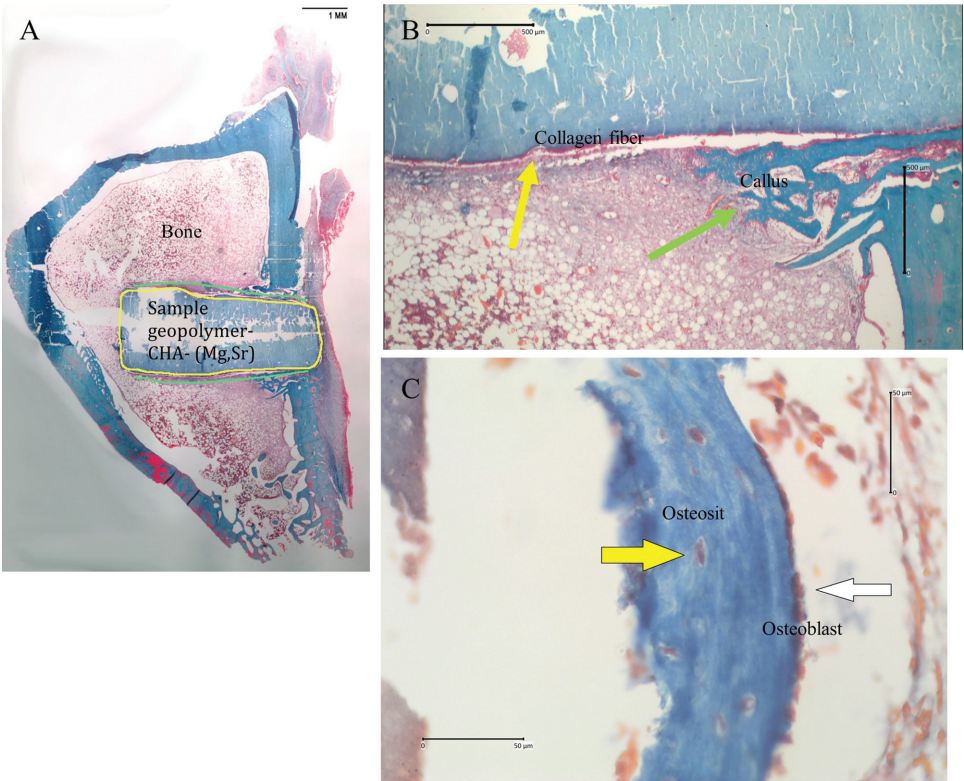
Fig. 6 Sample geopolymer-CHA-Mg-Sr with 3 mm in diameter and 6 mm in length was positioned in the tibia metaphysis. (A) The yellow line is the circumference of the implant, the green line is the length of newly formed collagen tissue, objective magnification ×40. (B) New collagen tissue (yellow arrow), new callus/bone tissue (green arrow), objective magnification ×4. (C) Osteocyte (yellow arrow); osteoblast (white arrow); bone (blue), objective magnification ×40. CHA, carbonated hydroxyapatite.

Table 3 The mean length of new collagen fiber formed in the geopolymer-CHA-Mg-Sr contact area with bone on days 14 and 28

Material	Length of collagen fiber (mm ± SD)	N	p-Value
Geopolymer-CHA-Mg-Sr-14	8.357 ± 0.614	4	0.075[a]
Geopolymer-CHA-Mg-Sr-28	10.268 ± 1.119	4	

Abbreviations: CHA, carbonated hydroxyapatite; SD, standard deviation.
[a]Significant ($p < 0.05$).

Table 4 The mean length of callus formed in the geopolymer-CHA-Mg-Sr contact area with bone on days 14 and 28

Material	Length of callus (mm ± SD)	N	p-Value
Geopolymer-CHA-Mg-Sr-14	0.713 ± 0.514	4	0.842[a]
Geopolymer-CHA-Mg-Sr-28	0.805 ± 0.466	4	

Abbreviations: CHA, carbonated hydroxyapatite; SD, standard deviation.
[a]Significant ($p < 0.05$).

In the proliferative phase, FGF triggers fibroblasts to secrete extracellular matrix proteins such as collagen, chondroitin sulfate, fibronectin, vitronectin, and other proteoglycans. These proteins guide osteoprogenitor cells to migrate toward the implant through the interaction of integrins on the cell surface.

In the remodeling phase, woven bone develops into trabecular bone, osteoblasts interact with osteoclasts. Sclerotin is a messenger molecule that mediates osteoblast–osteoclast interactions. Sclerotin is secreted by osteocytes (►**Fig. 6C**) and acts as an inhibitor of osteogenesis by blocking osteoblastic bone formation.[11]

The total contact area between implant and bone plays an important role in the osseointegration strength of the bone–implant interface, and this area is influenced by several factors such as surface treatment and implant material.[50]

Bone apposition must not be obtained 100% on the endosseous implant surface. Albrektsson and Johansson[51] showed that the proportion of direct bone-to-implant contact varies with implant material and design, the state of the

host bone, surgical technique, and loading time and conditions.[7]

The lack of a significant difference in collagen deposition (p-values of 0.075 and 0.842) in this study is more likely due to the limited observation time during the proliferative phase. During this phase (several weeks to months), the low wound strength is associated with the formation of collagen fibers of small diameter, later on days 28 until 45, an acute change appears corresponding to the remodeling phase, with increased collagen fiber diameters observed by scanning electron microscopy and light microscopy, increased tensile strength and toughness. Until day 90, the packing density of collagen fibrils was unchanged, although collagen fiber diameters increased during this time.[52]

Meanwhile, the sample size in this study was considered based on the manufacturer's standard implant size, critical defect size, and the anatomy of the rabbit tibia bone. Based on the standard size of the manufacturer's implant, the size of the implant in this study was 3.0 mm in diameter and 6.0 mm in length, similar to one of the products from Bicon's short implant system.

Based on the perspective of critical size defect, there are several considerations from the literature that underlie the selection of sample size based on critical size defect. According to the research by Meng et al, osteochondral defects with a diameter of 3.0 to 5.0 mm and a depth of 2.0 to 5.0 mm are often used to evaluate biomaterials in rabbit models.[53] According to Mapara et al, the implant size and length should be as small as possible. The recommended norm is 2 mm in diameter and 6 mm in length, as there is size limitation of rabbit bone. The smaller size of the implant also reduces the sequencing of drills and the drilling time.[54]

As stated by Pearce et al, the guidelines had been provided for the dimensions of implants for in vivo studies, based on the size of the animal and bone chosen and on the implant design, to avoid pathological fracture of the test site. Cylindrical implants placed into rabbit tibial and femoral diaphyseal bone should not be more than 2 mm in diameter and 6 mm in length.[55]

Based on the anatomy of rabbit tibia bone, guidelines are provided for the dimensions of implants for in vivo studies according to the size of the animal and bone chosen and on the implant design, to avoid pathological fracture of the test site. Cylindrical implants placed into rabbit tibial and femoral diaphyseal bone should not be more than 2 mm in diameter and 6 mm in length.[55]

Conclusion

Modern dentistry aims to restore patients to normal contour, function, comfort, esthetics, speech, and stomatognathic systems. The biocompatibility of synthetic biomaterials used for dental implants has always been a significant concern. For optimal performance, implant biomaterials must possess appropriate mechanical properties, biocompatibility, and structural biostability in physiological environments.

Dental implants are used in the oral cavity to enhance the stability of prostheses. To be clinically successful, the implant materials must meet two important requirements, first, the materials should not be toxic to the cells in the surrounding tissue or dissolve, causing systemic damage to the patient and second, they must be able to form a stable bone–implant interface capable of bearing occlusal loads and transferring or distributing pressure to the adjacent bone, thereby maintaining bone vitality over a long period.

The geopolymer-CHA-Mg-Sr was biocompatible. All samples showed cell viability values higher than 80% in biological characterization. It is noteworthy to mention here that all samples were biocompatible. After 72 hours of incubation, the cell viability reached higher than 90%, calculated at 95.7% for geopolymer-CHA-Mg-Sr.

Likewise, the mechanical properties meet the dentin standard values for hardness, while the modulus of elasticity, compressive, and tensile strength meet the enamel standard values.

The percentage of collagen tissue deposition formed on geopolymer-CHA-Mg-Sr on days 14 and 28 increased from 63.98 to 72.45%, while the rate of callus formation on days 14 and 28 was 8.13 and 7.80%, respectively.

Collagen fiber deposition and callus formation are significant for bone repair and regeneration success. One factor that determines the material's success is the presence of unimpeded bone growth on or across the surface of the material sample at the initial stage of the bone healing sequence, which is characterized by the deposition of collagen fiber and callus formation as shown on the surface of the geopolymer-CHA-Mg-Sr sample.

Although geopolymer-CHA-Mg-Sr meets biocompatible and mechanical properties, the results of collagen fiber deposition and callus formation have not shown significant outcomes.

Rabbits were used in this study because they are one of the commonly used animal models for screening implant materials before testing on higher level animals such as dogs, goats, sheep, and pigs. To observe a better response in collagen fiber deposition and callus formation, it is recommended to use higher level animal models such as dogs, goats, sheep, and pigs. Additionally, it is suggested to extend the observation period from the proliferation to the remodeling stage to improve the statistical power of future research.

References

1 Al-Molla BH, Al-Ghaban N, Taher A. In vivo immunohistochemical investigation of bone deposition at amelogenin coated Ti implant surface. Smile Dent J 2014;9(01):12–17

2 Saini M, Singh Y, Arora P, Arora V, Jain K. Implant biomaterials: a comprehensive review. World J Clin Cases 2015;3(01):52–57

3 Shi J, Li Y, Gu Y, Qiao S, Zhang X, Lai H. Effect of titanium implants with strontium incorporation on bone apposition in animal models: a systematic review and meta-analysis. Sci Rep 2017;7 (01):15563

4 Apratim A, Eachempati P, Krishnappa Salian KK, Singh V, Chhabra S, Shah S. Zirconia in dental implantology: a review. J Int Soc Prev Community Dent 2015;5(03):147–156

5 Chun KJ, Lee JY. Comparative study of mechanical properties of dental restorative materials and dental hard tissues in compressive loads. J Dent Biomech 2014;5(10):1758736014555246

6 Ramazanoglu M, Oshida Y. Osseointegration and bioscience of implant surface-current concepts at bone-implant interface. In IIser Turkyilmaz (Ed.) In: Implant Dentistry - A Rapidly Evolving Practice. Vol. 8. 2011:57–82

7 Isa ZM. Dental implants: biomaterial, biomechanical, and biological considerations. Annal Dent Univ Malaya 2000;7(01):27–35

8 Cui WF, Liu N, Qin GW. Microstructures, mechanical properties and corrosion resistance of the Zr e x Ti (Ag) alloys for dental implant application. J Mat Chem Phys 2016;(06):161–166

9 Sales A, Singh A, Zehra M, Naim H. Factors affecting osseointegration of dental implants: a review. J Int Dent Med Res 2023;16(03): 1272–1279

10 Łukaszewska-Kuska M, Krawczyk P, Martyla A, Hędzelek W, Dorocka-Bobkowska B. Effects of a hydroxyapatite coating on the stability of endosseous implants in rabbit tibiae. Dent Med Probl 2019;56(02):123–129

11 Smeets R, Stadlinger B, Schwarz F, et al. Review article impact of dental implant surface modifications on osseointegration. BioMed Res Int 2016;(07):1–16

12 Colombo JS, Satoshi S, Okazaki J, Crean SJ, Sloan AJ, Waddington RJ. In vivo monitoring of the bone healing process around different titanium alloy implant surfaces placed into fresh extraction sockets. J Dent 2012;40(04):338–346

13 Kuroda K, Okido M. Review article: hydroxyapatite coating of titanium implants using hydroprocessing and evaluation of their osteoconductivity. Bioinorg Chem Appl 2012;9(02):1–7

14 Xuereb M, Camilleri J, Attard NJ. Systematic review of current dental implant coating materials and novel coating techniques. Int J Prosthodont 2015;28(01):51–59

15 Goodman SB, Yao Z, Keeney M, Yang F. The future of biologic coatings for orthopaedic implants. Biomaterials 2013;34(13): 3174–3183

16 Wang H, Li H, Yan F. Synthesis and mechanical properties of metakaolinite-based geopolymer. Colloids Surf A Physicochem Eng Asp 2005;268(01):1–6

17 Catauro M, Bollino F, Papale F, Lamanna G. Investigation of the sample preparation and curing treatment effects on mechanical properties and bioactivity of silica rich metakaolin geopolymer. Mater Sci Eng C 2014;36(12):20–24

18 Sauffi AS, Mastura W, Ibrahim W, Mustafa M, Bakri A. A review of carbonate minerals as an additive to geopolymer materials a review of carbonate minerals as an additive to geopolymer materials. Mater Sci Eng 2019;551(01):012084

19 Chen L, Wang Z, Wang Y, Feng J. Preparation and properties of alkali activated metakaolin-based geopolymer. Materials (Basel) 2016;9(09):1–12

20 Rovnanik P. Effect of Curing temperature on the development of hard structure of metakaolin-based geopolymer. Constr Build Mater 2014;24(07):1176–1183

21 Muslimin H, Pane I, Imran I, Budiono B. Compressive strength of fly ash-based geopolymer concrete with a variable of sodium hydroxide (NaOH) solution molarity. MATEC Web Conf 2018;147 (01):01004

22 Blaszczynski T, Król M. Alkaline activator impact on the geopolymer binders. IOP Conf Series Mater Sci Eng 2017;245(02): 022036

23 Catauro M, Bollino F, Kansal I, Kamseu L, Lancellotti I, Leonelli C. Mechanical and biological characterization of geopolymers for potential application as biomaterials. Azo J Mater 2012;(05): 0322

24 Tippayasam C, Sutikulsombat C, Kamseu E, et al. In vitro surface reaction in sbf of a non-crystalline aluminosilicate (geopolymer) material. J Aust Ceram Soc 2018;55(06):11–17

25 Okayama S, Akao M, Nakamura S, Shin Y, Higashikata M, Aoki H. The mechanical properties and solubility of strontium-substituted hydroxyapatite. Biomed Mater Eng 1991;1(01):11–17

26 LeGeros RZ, Kijkowska R, Bautista C, LeGeros JP. Synergistic effects of magnesium and carbonate on properties of biological and synthetic apatites. Connect Tissue Res 1995;33(1-3):203–209

27 Boyd AR, Rutledge L, Randolph LD, Meenan BJ. Strontium-substituted hydroxyapatite coatings deposited via a co-deposition sputter technique. Mater Sci Eng C 2015;46(01):290–300

28 Landi E, Sprio S, Sandri M, Celotti G, Tampieri A. Development of Sr and CO3 co-substituted hydroxyapatites for biomedical applications. Acta Biomater 2008;4(03):656–663

29 Yang F, Yang D, Tu J, Zheng Q, Cai L, Wang L. Strontium enhances osteogenic differentiation of mesenchymal stem cells and in vivo bone formation by activating Wnt/catenin signaling. Stem Cells 2011;29(06):981–991

30 Saidak Z, Marie PJ. Strontium signaling: molecular mechanisms and therapeutic implications in osteoporosis. Pharmacol Ther 2012;136(02):216–226

31 Li M, He P, Wu Y, et al. Stimulatory effects of the degradation products from Mg-Ca-Sr alloy on the osteogenesis through regulating ERK signaling pathway. Sci Rep 2016;6(06):32323

32 Marsell R, Einhorn TA. The biology of fracture healing. Injury 2011;42(06):551–555

33 Terheyden H, Lang NP, Bierbaum S, Stadlinger B. Osseointegration–communication of cells. Clin Oral Implants Res 2012;23(10): 1127–1135

34 Loi F, Córdova LA, Pajarinen J, Lin TH, Yao Z, Goodman SB. Inflammation, fracture and bone repair. Bone 2016;86(03): 119–130

35 Ghiasi MS, Chen J, Vaziri A, Rodriguez EK, Nazarian A. Bone fracture healing in mechanobiological modeling: a review of principles and methods. Bone Rep 2017;6(03):87–100

36 Mescher AL. Junqueira's Basic Histology. 15th ed. New York: McGraw Hill; 2018:103–104,145,148

37 Chun K, Choi H, Lee J. Comparison of mechanical property and role between enamel and dentin in the human teeth. J Dent Biomech 2014;5(01):1758736014520809

38 Marshall GW Jr, Marshall SJ, Kinney JH, Balooch M. The dentin substrate: structure and properties related to bonding. J Dent 1997;25(06):441–458

39 Park S, Wang DH, Zhang D, Romberg E, Arola D. Mechanical properties of human enamel as a function of age and location in the tooth. J Mater Sci Mater Med 2008;19(06):2317–2324

40 Sharma A, Ahmad J. Factors affecting compressive strength of geopolymer concrete-a review. IRJET 2017;4(04):2026–2031

41 Cho S. Geopolymer Composites and Their Applications in Stress Wave Mitigation. University of Illinois at Urbana-Champaign 2015:1–139

42 Zreiqat H, Howlett CR, Zannettino A, et al. Mechanisms of magnesium-stimulated adhesion of osteoblastic cells to commonly used orthopaedic implants. J Biomed Mater Res 2002;62 (02):175–184

43 Bose S, Fielding G, Tarafder S, Bandyopadhyay A. Understanding of dopant-induced osteogenesis and angiogenesis in calcium phosphate ceramics. Trends Biotechnol 2013;31(10):594–605

44 Castiglioni S, Cazzaniga A, Albisetti W, Maier JAM. Magnesium and osteoporosis: current state of knowledge and future research directions. Nutrients 2013;5(08):3022–3033

45 Díaz-Tocados JM, Herencia C, Martínez-Moreno JM, et al. Magnesium chloride promotes osteogenesis through notch signaling

activation and expansion of mesenchymal stem cells. Sci Rep 2017;7(01):7839

46 Zhao SF, Jiang QH, Peel S, Wang XX, He FM. Effects of magnesium-substituted nanohydroxyapatite coating on implant osseointegration. Clin Oral Implants Res 2013;24(08, suppl A100):34–41

47 Boskey AL. Bone composition: relationship to bone fragility and antiosteoporotic drug effects. Bonekey Rep 2013;2(12):447

48 Tao ZS, Zhou WS, He XW, et al. A comparative study of zinc, magnesium, strontium-incorporated hydroxyapatite-coated titanium implants for osseointegration of osteopenic rats. Mater Sci Eng C 2016;62(05):226–232

49 Tan S, Zhang B, Zhu X, et al. Deregulation of bone forming cells in bone diseases and anabolic effects of strontium-containing agents and biomaterials. BioMed Res Int 2014;2014(03):814057

50 Lan TH, Du JK, Pan CY, Lee HE, Chung WH. Biomechanical analysis of alveolar bone stress around implants with different thread designs and pitches in the mandibular molar area. Clin Oral Investig 2012;16(02):363–369

51 Albrektsson T, Johansson C. Quantified bone tissue reactions to various metallic materials with reference to the so-called osseointegration concept. In: Davies JE, ed. The Bone-Biomaterial Interface. Toronto: University of Toronto Press; 1991:357–363

52 Doillon CJ, Dunn MG, Bender E, Silver FH. Collagen fiber formation in repair tissue: development of strength and toughness. Coll Relat Res 1985;5(06):481–492

53 Meng X, Ziadlou R, Grad S, et al. Animal models of osteochondral defect for testing biomaterials. Biochem Res Int 2020;2020(01): 9659412

54 Mapara M, Thomas BS, Bhat KM. Rabbit as an animal model for experimental research. Dent Res J (Isfahan) 2012;9(01):111–118

55 Pearce AI, Richards RG, Milz S, Schneider E, Pearce SG. Animal models for implant biomaterial research in bone: a review. Eur Cell Mater 2007;13(03):1–10